IEEE Access
Multidisciplinary | Rapid Review | Open Access Journal

Received March 19, 2019, accepted April 7, 2019, date of publication April 12, 2019, date of current version April 26, 2019.

Digital Object Identifier 10.1109/ACCESS.2019.2910936

Adaptive Backstepping Sliding Mode Control for Boost Converter With Constant Power Load

JIARONG WU AND YIMIN LU, (Member, IEEE)
School of Electrical Engineering, Guangxi University, Nanning 530004, China

Corresponding author: Yimin Lu (y.m.lu@gxu.edu.cn)

This work was supported in part by the National Natural Science Foundation of China under Grant 51667005, and in part by the Natural Science Foundation of Guangxi Province under Grant 2018GXNSFDA281037.

ABSTRACT The negative impedance characteristics of a constant power load (CPL) can easily lead to the instability of the DC bus voltage. To improve the stability of the DC bus voltage, an adaptive backstepping sliding mode control strategy for a boost converter with the CPL in DC microgrid is proposed. First, to carry out the backstepping control, the zero dynamic stability of the system under different output functions is studied by using input–output exact feedback linearization theory. The model is transformed into a linear system in Brunovsky canonical form, which solves the nonlinear problem caused by the CPL and the non-minimum phase problem of the boost converter. Then, under the premise of ensuring large signal stability, an adaptive mechanism is introduced into the design of the backstepping sliding mode control. The adaptive backstepping sliding mode controller is designed by adaptively updating the switching gain in real time. Furthermore, the Lyapunov theory is used to prove the global asymptotic stability of the overall closed-loop system. Finally, the numerical simulation and experimental results show that the proposed control strategy has better dynamic regulation performance and stronger robustness compared with the conventional double closed-loop PI control method.

INDEX TERMS Constant power load, boost converter, exact feedback linearization, backstepping sliding mode control adaptive.

I. INTRODUCTION

With the growth of energy demand and the depletion of traditional fossil energy, renewable energy has received more and more attention. In recent years, the massive integration of renewable energy and the increasing number of electronic loads have made DC distribution systems and DC microgrids options for building more efficient and portable systems. The DC microgrid not only has the advantages of a high overall system efficiency and easy connection with renewable energy and consumer electronics but also is exempted from problems of frequency synchronization, reactive current, and phase imbalance compared with AC microgrids. Therefore, DC microgrids have been widely used in electrical energy systems [1]. In a DC microgrid, a large number of electronic loads are connected to the DC bus. When the load is controlled to output a constant power, it behaves as a constant power load (CPL). In DC power systems, CPLs exist in automotive systems and space power systems in the form of distributed power or motor drives [2]. In the field of avionics, nearly 75% of aircraft loads show CPL characteristics [3]. Therefore, the stability and reliability of DC microgrids with CPL have become the focus of attention [4], [5].

Maintaining the stability of the DC bus voltage is a key issue to ensuring the stability of the DC microgrid. However, the CPL has negative impedance characteristics [6], [7], which reduces the damping coefficient of the system, resulting in the instability of the DC bus voltage. In addition, the DC microgrid with CPL is a typical switching nonlinear system, posing great limitations to the direct application of linear control methods in the design of such system controllers. In recent years, the exact feedback linearization (EFL) method, developed from the differential geometry theory [8], has successfully solved the problem of converting nonlinear systems to linear systems. Moreover, the linearization process does not ignore any higher-order nonlinear terms. Thus, the EFL method has been widely used in the control of power electronic switching converters [9], [10]. In [10], the control of a three-phase AC/DC voltage source converter is implemented by using the input-output EFL method.

The associate editor coordinating the review of this manuscript and approving it for publication was Ludovico Minati.

However, most of the EFL control methods are based on assumptions of the exact mathematical model of the nonlinear system, without considering the uncertainty of the actual system parameters or the influence of external disturbances on the system. Additionally, this method cannot be directly applied to systems with unstable zero dynamics [11]. Therefore, when the system does not meet the conditions of exact linearization, it is also necessary to consider the stability of zero dynamics; otherwise, the system may be non-minimum phase, resulting in negative regulation characteristics [12]. This deteriorates the dynamic quality of the control system, resulting in a prolonged system transition time. In the negative regulation period, the controller receives the opposite feedback signal to form a positive feedback system, seriously affecting the transient performance and steady-state performance of the system.

To solve the instability problem of DC-DC converters caused by CPLs, researchers have proposed numerous control algorithms. A bus voltage stability control method based on state feedback linearization [2] is proposed to ensure the stability of the multi-converter DC power supply system with a CPL. A loop cancellation technique [3] is proposed to overcome the unstable effects of DC-DC converters caused by CPLs. Based on the EFL theory, the system is made into a minimum phase system in [11] by injecting a small-signal inductor current at the output node to facilitate controller design. A current control strategy [13] for boost converters with CPL is proposed, and the stability of the system is analyzed in the context of a small signal model. In [14], the dynamic stability of a DC microgrid with a CPL is analyzed, and then model predictive control is proposed to control the CPL, making the system robust. A passive controller [15] for an adaptive damping distribution for the boost converter with a CPL under a DC microgrid is proposed. The control algorithm ensures the stability and fast response of the system under different modes when the load changes. In [16], based on the EFL of the buck converter with a CPL, a control method combining feedback control and feedforward control strategies is used to control the system, improving the dynamic performance. A passive damping control method [17] is proposed to effectively convert a CPL into a resistive load, thus avoiding the influence of the CPL negative impedance characteristics but greatly reducing the efficiency of the system due to its large volume. Active damping control methods are mentioned in [18] and [19]. In [19], a compensation current is added to the CPL to modify the control structure, and a capacitor power component is added to the CPL to alleviate the impact of the CPL. The stability control problem of the DC microgrid under a CPL is studied in [20], and a Kalman filter and robust feedback controller are proposed to improve the robustness of the system. A control strategy combining a nonlinear disturbance observer (NDO) and backstepping control [21] is proposed for the boost converter with a CPL under a DC microgrid to improve the dynamic response of the system.

The above algorithms solve the instability problem of the DC-DC converter with a CPL to some extent. However, when the system has unstable zero dynamics, or the mathematical model is not accurate, further research on more robust methods is needed to ensure the normal operation of the system. Sliding mode control (SMC) method receives much attention in power electronic converter due to its strong robustness to external disturbances, unmodeled dynamics and parameter uncertainties [22]–[28]. A sliding mode duty-cycle controller (SMDC) [22] is applied to a buck converter with a CPL to enable the system to operate stably over the entire operating range in the presence of significant changes in the load power and input voltage. A robust pulse width modulation sliding mode controller [23] is proposed, in which a new nonlinear curved surface is adopted to ensure the stability of the converter system with a CPL. Although SMC can suppress the influence of system parameter changes on the system, the use of a fixed sliding mode gain may result in a strong chatter phenomenon. Additionally, SMC is a control technique that requires internal dynamic stability [11]; however, whether the system zero dynamics is stable has not been studied in the literature. In recent years, the backstepping sliding mode control (BSMC) method has been highly valued for its complete adaptability to system disturbances and parameter perturbation [29], [30]. This method based on step-by-step backstepping algorithm with strictly guaranteed large signal stability avoids the impact of unstable zero dynamics on the system. An improved BSMC method based on error compensation [30] is proposed for the nonlinear power system of the generator steam valve, achieving good results for suppressing system disturbances. However, to determine the switching gain of the BSMC, it is necessary to acquire in advance the upper bound information of the parameter uncertainty and external disturbance. Since such information cannot be obtained in most cases, severe chatter may occur if a conservative method is used to select a large switching gain to ensure the stability of the system [30].

To address the above problems, this paper proposes a nonlinear control strategy that combines the EFL technique and the adaptive backstepping sliding mode control (ABSMC). For the instability caused by the CPL, the original nonlinear system is transformed into a linear system in Brunovsky canonical form by the EFL technique, facilitating the design of the BSMC. Then, the adaptive mechanism is introduced into the BSMC to solve the problem that the traditional BSMC cannot estimate a priori the upper bound information of the disturbance and the system parameter uncertainty, reducing the influence of the chatter on the system. Taking the boost converter with a CPL as the control object, the design steps of the proposed control strategy are analyzed in detail. Finally, the superiority and correctness of the proposed control strategy is verified by simulation and experiment.

The paper is organized as follows. In part II, the affine nonlinear model of boost converter with CPL in DC microgrid is established. In part III, the zero dynamic stability of the system under different output functions is discussed based

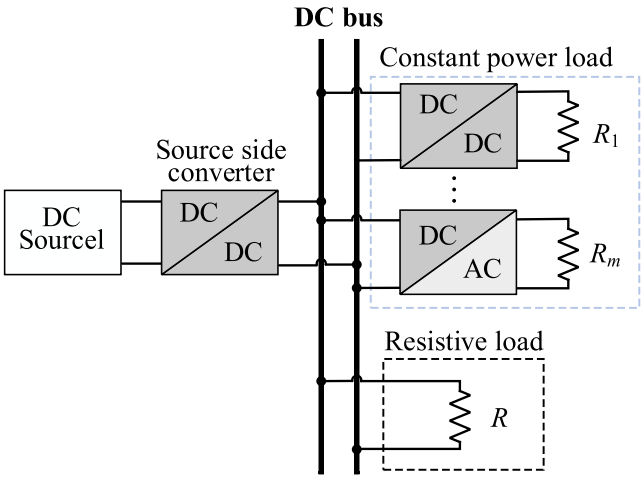

FIGURE 1. A typical DC microgrid.

on EFL theory. In part IV, the ABSMC strategy is proposed based on the transformation of the original nonlinear system to a linear system in Brunovsky canonical form, and the global asymptotic stability of the closed-loop system is proved based on the Lyapunov stability theory. In parts V, the numerical simulation between the proposed control strategy and the conventional double closed-loop PI control strategy is carried out, and the simulation results verify the superiority and correctness of the proposed control strategy. In parts VI, the experiments on the proposed control strategy is carried out, and the experimental results verify the feasibility of the proposed control strategy. The conclusions are presented in part VII.

II. SYSTEM DESCRIPTION AND ITS AFFINE NONLINEAR MODEL

Fig.1 shows a typical DC microgrid structure [31]. The DC source provides the required voltage for the DC bus through a DC-DC converter, and a large number of electronic loads, such as the controlled rectifier or the inverter, connected to the DC bus can be regarded as CPLs. The bus voltage provides not only a constant voltage for the resistive load but also a constant power to the CPLs to ensure the proper operation of the various loads. The negative impedance characteristics of the CPL and the changes in the load or distributed power supply can cause fluctuations in the DC bus voltage and even the instability of the entire DC microgrid.

Fig.2 shows a simplified DC distribution system. In the system, the distributed power supply provides voltage to the DC bus through a boost converter, and the resistive load and the CPL are connected in parallel to the DC bus. V_{in} is the total input voltage of the distributed power supply, L is the filter inductor, C is the filter capacitor, R is the total resistive load, v_{C} is the capacitor voltage, i.e., bus voltage, i_{L} is the filter inductor current, P is the lumped constant power load, i_{o} is the output current, D is the diode, Q is the switching

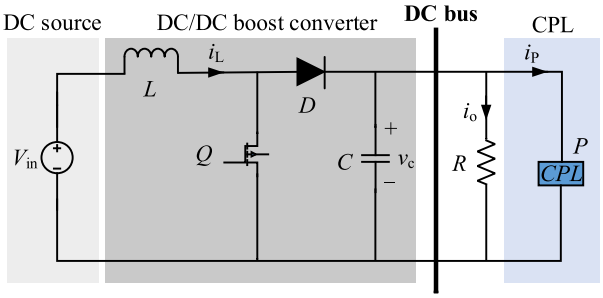

FIGURE 2. The simplified DC distribution system.

device. The voltage-current characteristics of a CPL is given by $i_{\text{P}} = P / v_{\text{C}}$, where i_{P} is the instantaneous values of input current of the CPL.

Assuming that the system works in continuous current mode (CCM), the average model of the boost converter with CPL shown in Fig. 2 is established by state space averaging:

$$\begin{cases} \dfrac{di_{\text{L}}}{dt} = \dfrac{V_{\text{in}} - v_{\text{c}}}{L} + \dfrac{v_{\text{c}}}{L}d \\ \dfrac{dv_{\text{c}}}{dt} = \dfrac{1}{C}\left(i_{\text{L}} - \dfrac{v_{\text{c}}}{R} - \dfrac{P}{v_{\text{c}}}\right) - \dfrac{i_{\text{L}}}{C}d \end{cases} \tag{1}$$

where d is the duty cycle. Equations (1) shows that the system is a nonlinear system.

For a general single-input single-output affine nonlinear system:

$$\begin{cases} \dot{x} = f(x) + g(x)u \\ y = h(x) \end{cases} \tag{2}$$

where $\boldsymbol{x} = [x_1, x_2, \ldots, x_n]^{\text{T}}$, u and y represent the state, input and output of the system, respectively, n is the dimension of the system.

Comparing (1) and (2), the boost converter with a CPL is a canonical affine nonlinear system, in which

$$f(x) = \begin{bmatrix} \dfrac{V_{\text{in}} - x_2}{L} \\ \dfrac{x_1}{C} - \dfrac{x_2}{CR} - \dfrac{P}{Cx_2} \end{bmatrix} \quad \text{g}(x) = \begin{bmatrix} \dfrac{x_2}{L} \\ -\dfrac{x_1}{C} \end{bmatrix} \tag{3}$$

where $[x_1, x_2] = [i_{\text{L}}, v_{\text{C}}]$, $u = d$.

III. INTERNAL STABILITY ANALYSIS OF SYSTEM UNDER DIFFERENT OUTPUT FUNCTIONS

For a particular nonlinear system, when the system does not meet the full linearization condition, the system will have unstable zero dynamics, making the system a non-minimum phase system. Therefore, it is necessary to discuss the zero-dynamic stability of the system. The conditions for the system to be fully linearized are given below. For the affine nonlinear system shown in (2), if the following two conditions are true:

1) The rank of matrix $[g(\boldsymbol{x})\ ad_f g(\boldsymbol{x})\ \ldots ad_f^{n-2} g(\boldsymbol{x})\ ad_f^{n-1} g(\boldsymbol{x})]$, for all $\boldsymbol{x}$ near $\boldsymbol{x}_0$, is constant and equal to n; and
2) The set of vector fields $\boldsymbol{B}= \{g(\boldsymbol{x}),\ ad_f g(\boldsymbol{x}),\ \ldots,\ ad_f^{n-2} \text{g}(\boldsymbol{x})\}$ are coincident at $\boldsymbol{x}= \boldsymbol{x}_0$,

where $ad_f g(\boldsymbol{x})$ represents the Lie bracket of the vector field $g(\boldsymbol{x})$ and another vector field $f(\boldsymbol{x})$, then there must exist a function $\eta(\boldsymbol{x})$ such that the degree of relationship r of the system at$\boldsymbol{x}=\boldsymbol{x}_0$ is equal to the dimension n of the system, i.e., the given system can be accurately linearized on an open set of $\boldsymbol{x}=\boldsymbol{x}_0$ into a controllable linear system — Brunovsky canonical form [8].

The zero dynamic stability of the system under different output functions is studied below.

A. INTERNAL STABILITY ANALYSIS UNDER CAPACITOR VOLTAGE

Take the capacitor voltage as the output function:

$$h_1(\boldsymbol{x}) = x_2 \tag{4}$$

$$L_g h_1(\boldsymbol{x}) = \frac{\partial h_1(\boldsymbol{x})}{\partial \boldsymbol{x}} g(\boldsymbol{x}) = -\frac{x_1}{C} \neq 0 \tag{5}$$

where $L_g h_1(\boldsymbol{x})$ represents the Lie derivative of the output function $h_1(\boldsymbol{x})$ with respect to vector field $g(\boldsymbol{x})$. The degree of relationship is $r = 1$, which is less than the dimension $n = 2$ of the system. Therefore, by controlling the capacitor voltage, the system can only achieve partial linearization. For this reason, it is also necessary to verify the zero-dynamic stability of the system.

To complete the coordinate transformation, let $\xi_1 = x_2$. According to the input-output EFL theory, the function $\eta_1(\boldsymbol{x})$ corresponding to the internal dynamics satisfies the relationship $L_g \eta_1(\boldsymbol{x}) = 0$, and one of the solutions $\eta_1(\boldsymbol{x})$ is:

$$\eta_1(\boldsymbol{x}) = \frac{1}{2} L x_1^2 + \frac{1}{2} C x_2^2 \tag{6}$$

Thus, the internal dynamic equation of the system is:

$$\dot{\eta}_1 = V_{\text{in}} \sqrt{\frac{L}{2}(\eta_1 - \frac{1}{2} C \xi_1^2)} - \frac{\xi_1^2}{R} - P \tag{7}$$

Let the zero dynamics of the system at $\xi_1 = 0$ be:

$$\dot{\eta}_1 = V_{\text{in}} \sqrt{\frac{2\eta_1}{L}} - P \tag{8}$$

According to (8), an equilibrium point and the Jacobian matrix can be calculated as: $Q_1 = LP^2/(2V_{in}^2)$ and $\partial \dot{\eta}_1 / \partial \eta_1 = V_{\text{in}}/(\sqrt{2\eta_1 L})$, respectively. Then the eigenvalue of (8) at the Q_1 can be obtained as: $\lambda_1 = V_{\text{in}}^2/(PL)$ which is located in the right-half complex plane, thus the zero dynamics shown in (8) are unstable. Therefore, it is a non-minimum phase system when the capacitor voltage is used as the system output feedback value.

B. INTERNAL STABILITY ANALYSIS UNDER INDUCTOR CURRENT

Take the inductor current as the output function:

$$h_2(\boldsymbol{x}) = x_1 \tag{9}$$

The system can only achieve partial linearization. By using the internal dynamic function $\eta_2(\boldsymbol{x}) = \eta_1(\boldsymbol{x})$, which is consistent with the capacitor voltage, the zero dynamic of the system can be obtained as:

$$\dot{\eta}_2 = -\frac{2}{CR} \eta_2 - P \tag{10}$$

An eigenvalue of (10) can be obtained as: $\lambda_2 = -2/(CR)$ which is located in the left-half complex plane, thus the zero dynamics shown in (10) are stable. It is a minimum phase system. Therefore, the stability of the bus voltage can be indirectly controlled by controlling the inductor current.

IV. ADAPTIVE BACKSTEPPING SLIDING MODE CONTROL

It can be seen from the above analysis that although the stability of the bus voltage can be indirectly controlled by controlling the inductor current, the problems of indirect regulation are that the system cannot form an output response and that the bus voltage response changes with the open-loop dynamics, resulting in a slower response and excessive overshoot [9]. Therefore, the output function $h(\boldsymbol{x})$ must be redefined to meet the requirements for full linearization. From the above analysis, $h(\boldsymbol{x})$ can be taken as:

$$h(\boldsymbol{x}) = \frac{1}{2} L x_1^2 + \frac{1}{2} C x_2^2 \tag{11}$$

Therefore, the coordinate transformation can be taken as:

$$\begin{cases} z_1 = h(\boldsymbol{x}) = \frac{1}{2} L x_1^2 + \frac{1}{2} C x_2^2 \\ z_2 = L_f h(\boldsymbol{x}) = V_{\text{in}} x_1 - \frac{x_2^2}{R} - P \end{cases} \tag{12}$$

After the coordinate transformation, the original nonlinear system can be transformed into the following linear system in Brunovsky canonical form:

$$\begin{cases} \dot{z}_1 = z_2 \\ \dot{z}_2 = v \end{cases} \tag{13}$$

where z_1 and z_2 are state variables of transformed linear systems, v is a new control variable and it has the following relationship with the control variable d of the original nonlinear control system (1):

$$d = \frac{-\alpha(\boldsymbol{x}) + v}{\beta(\boldsymbol{x})} \tag{14}$$

where

$$\begin{cases} \alpha(\boldsymbol{x}) = L_f^2 h(\boldsymbol{x}) = \frac{V_{\text{in}}(V_{\text{in}} - x_2)}{L} - \frac{2x_2}{RC}\left(x_1 - \frac{x_2}{R} - \frac{P}{x_2}\right) \\ \beta(\boldsymbol{x}) = L_g L_f h(\boldsymbol{x}) = \frac{V_{\text{in}} x_2}{L} + \frac{2x_1 x_2}{RC}. \end{cases}$$

Considering the uncertainty of the converter coefficient or the influence of external disturbances, the model established by (13) is inaccurate, and Equation (13) can be rewritten as:

$$\begin{cases} \dot{z}_1 = z_2 \\ \dot{z}_2 = \alpha(\boldsymbol{x}) + \beta(\boldsymbol{x}) \cdot d + F(t) \end{cases} \tag{15}$$

where $F(t)$ is the overall uncertainty of the uncertainty term and external disturbances.

Assumption: The system disturbance and the uncertainty term $F(t)$ is bounded, that is, $|F(t)| < F(t)_{\max}$ holds, where $F(t)_{\max}$ is an unknown positive constant.

The traditional backstepping control method cannot guarantee the robustness. The introducing of the sliding mode term can overcome the disturbances and guarantee the robustness of the controller [32]. To this end, the ABSMC algorithm is designed, with the control objective of making the system accurately track the target value under the influence of $F(t)$.

According to the backstepping design idea, first the tracking error and its first derivative are defined as:

$$e_1 = z_1 - z_{1\mathrm{d}} \tag{16}$$

$$\dot{e}_1 = z_2 - \dot{z}_{1\mathrm{d}} \tag{17}$$

where $z_{1\mathrm{d}}$ is the reference value of z_1, z_2 can be regarded as a virtual control variable.

To make $\dot{e}_1 = -c_1 e_1$(c_1 is a positive constant to be designed), one can let:

$$\alpha = \dot{z}_{1\mathrm{d}} - c_1 e_1 \tag{18}$$

To find the conditions that $z_2 - \alpha$tends to zero, the second error variable is defined as:

$$e_2 = z_2 - \alpha \tag{19}$$

By substituting (18) and (19) into (17), the first derivative of e_1 can be obtained as:

$$\dot{e}_1 = e_2 - c_1 e_1 \tag{20}$$

1) Select the Lyapunov function as:

$$V_1 = 0.5 e_1^2 \tag{21}$$

$$\dot{V}_1 = e_1 e_2 - c_1 e_1^2 \tag{22}$$

if $e_2 = 0$, then $\dot{V}_1 \leq 0$. To do this, the next step design is needed.

The derivative form of e_2 is:

$$\dot{e}_2 = \alpha(\boldsymbol{x}) + \beta(\boldsymbol{x}) \cdot d + F(t) - \ddot{z}_{1\mathrm{d}} + c_1 \dot{e}_1 \tag{23}$$

2) Select the Lyapunov function as:

$$V_2 = V_1 + 0.5 e_2^2 \tag{24}$$

$$\dot{V}_2 = e_1 e_2 - c_1 e_1^2 + e_2 \left(\alpha(\boldsymbol{x}) + \beta(\boldsymbol{x}) \cdot d + F(t) - \ddot{z}_{1\mathrm{d}} + c_1 \dot{e}_1\right) \tag{25}$$

According to sliding mode control theory, select the sliding mode surface:

$$s = e_2 \tag{26}$$

The sliding mode approach law [33] is selected as:

$$\dot{s} = -k_1 sgn(s) - k_2 s \tag{27}$$

where $k_2 > 0$ is the parameter which controls the convergence speed and $k_1 > 0$, which depends on the magnitude of uncertainty.

Combining (25), (26) and (27), the control law can be designed as:

$$d = \frac{-\alpha(\boldsymbol{x}) - e_1 + \ddot{z}_{1d} - c_1 \dot{e}_1 - k_1 sgn(s) - k_2 s}{\beta(\boldsymbol{x})} \tag{28}$$

Substitute (28) into (25), the results can be obtained as:

$$\dot{V}_2 = -c_1 e_1^2 - k_2 e_2^2 + e_2 F(t) - k_1 |e_2| \tag{29}$$

According to the working principle and actual working conditions of the boost converter with a CPL, the variation of the filter inductor, capacitor and load is limited; thus, $F(t)$ has an upper bound, and let $F(t) \leq K$, where K is the upper bound of $F(t)$. To ensure the stability of the system, select the control parameter $K \leq k_1$. From (29):

$$\begin{aligned} \dot{V}_2 &= -c_1 e_1^2 - k_2 e_2^2 + e_2 F(t) - k_1 |e_2| \\ &\leq -c_1 e_1^2 - k_2 e_2^2 - [k_1 - F(t)] |e_2| \\ &\leq 0 \end{aligned} \tag{30}$$

According to the Lyapunov stability theory, the system is asymptotically stable at $(e_1, e_2) = (0, 0)$ from (24) and (30)

However, the selection of the switching gain k_1 in the above design depends on the upper bound K of $F(t)$. If a conservative approach is adopted by choosing a sufficiently large switching gain k_1 to ensure system stability, severe chatter may occur. Therefore, the switching gain is updated in real time through the adaptive mechanism [34], effectively solving the switching gain selection problem. Let $\hat{k}_1$denote the estimated value of K, and its dynamic equation is

$$\hat{k}_1 = \varepsilon \int_0^t |s| d\tau \tag{31}$$

where $\varepsilon > 0$. According to (26), (27) and (31), reachability condition [35]

$$\begin{aligned} s\dot{s} &= -\varepsilon \int_0^t |s| d\tau sgn(s) s - k_2 s^2 \\ &= -\varepsilon \int_0^t |s| d\tau \, |s| - k_2 s^2 \\ &< 0 \end{aligned} \tag{32}$$

is satisfied. Then, the adaptive control law obtained by (28) is:

$$d = \frac{-\alpha(\boldsymbol{x}) - e_1 + \ddot{z}_{1\mathrm{d}} - c_1 \dot{e}_1 - \hat{k}_1 sgn(s) - k_2 s}{\beta(\boldsymbol{x})} \tag{33}$$

To verify the system shown in (15), the control law in (33) and the adaptive law in (31) are used, and the closed-loop system is asymptotically stable.

3) Select the Lyapunov function as below:

$$V_3 = V_2 + \frac{1}{2\varepsilon}(\hat{k}_1 - K)^2 \tag{34}$$

$$\begin{aligned} \dot{V}_3 &= -c_1 e_1^2 - k_2 e_2^2 + e_2 F(t) - \hat{k}_1 e_2 sgn(s) + \frac{1}{\varepsilon}\left(\hat{k}_1 - K\right)\dot{\hat{k}}_1 \\ &= -c_1 e_1^2 - k_2 e_2^2 + e_2 F(t) - K |e_2| \\ &\leq -c_1 e_1^2 - k_2 e_2^2 - [K - F(t)] |e_2| \\ &\leq 0 \end{aligned} \tag{35}$$

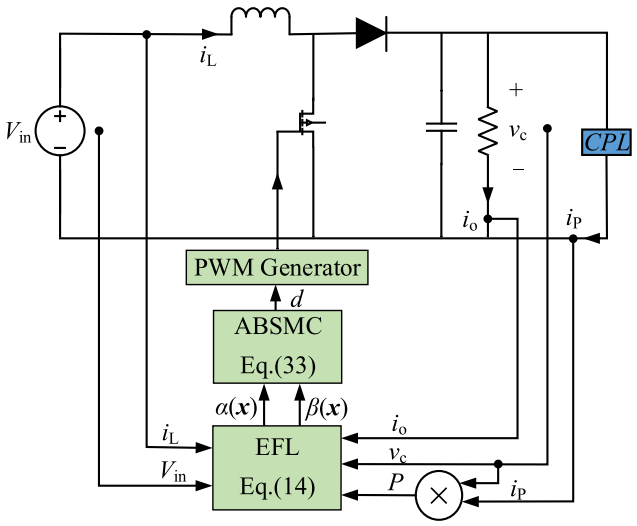

FIGURE 3. Adaptive backstepping sliding mode control block diagram.

Then, the system (15) is globally asymptotically stable, thereby completing the design of the proposed nonlinear controller. The dynamic quality of the system can be improved by adjusting the values for parameters c_1, ε, and k_2. Its control block diagram is shown in Fig. 3.

V. SIMULATION

To verify the effect of the proposed nonlinear control strategy, a system simulation model was built in this study on the MATLAB/Simulink platform, as shown in Fig. 3. The parameters of the system used for the simulation are listed as: $V_{in} = 12$ V,$V_{cref} = 24$ V, $L = 1$ mH, $C = 100$ μF, $R = 50\Omega$, $f_s = 50$ kHz and $P = 10$ W, which a closed - loop buck converter control system was connected to the aforementioned boost converter in cascades as a CPL. The controller parameters are set as $c_1 = 5000$, $k_2 = 7000$ and $\varepsilon = 50$.

To illustrate the superiority of the proposed nonlinear control strategy, the conventional double closed-loop PI control method is implemented for the boost converter with CPL with inner current loop and outer voltage loop. As PI parameters have impact on stability and dynamic response of the system, faster dynamics will lead to less stability margin. In the conventional double closed-loop PI controller, bandwidth frequency of the inner loop should be far higher than that of the outer loop. Generally, the bandwidth frequency for the inner current loop is set to at least 5 to 10 times that of the outer voltage loop. The bandwidth frequency of the inner current loop is constrained by and required to be far lower than the switching frequency. It is generally lower than 1/5–1/10 of the switching frequency. [36]. Here, the PI parameters for the inner current loop and the outer voltage loop are selected as: $k_{cp} = 2.66$, $k_{ci} = 700$ and $k_{vp} = 0.08$, $k_{vi} = 139$, respectively.

Fig. 4 shows the dynamic response waveform of the system when P is hopped from 10 W to 1 W, 1 W to 10 W and 10 W to 65 W at 0.06 s, 0.08 s and 0.10 s, respectively.

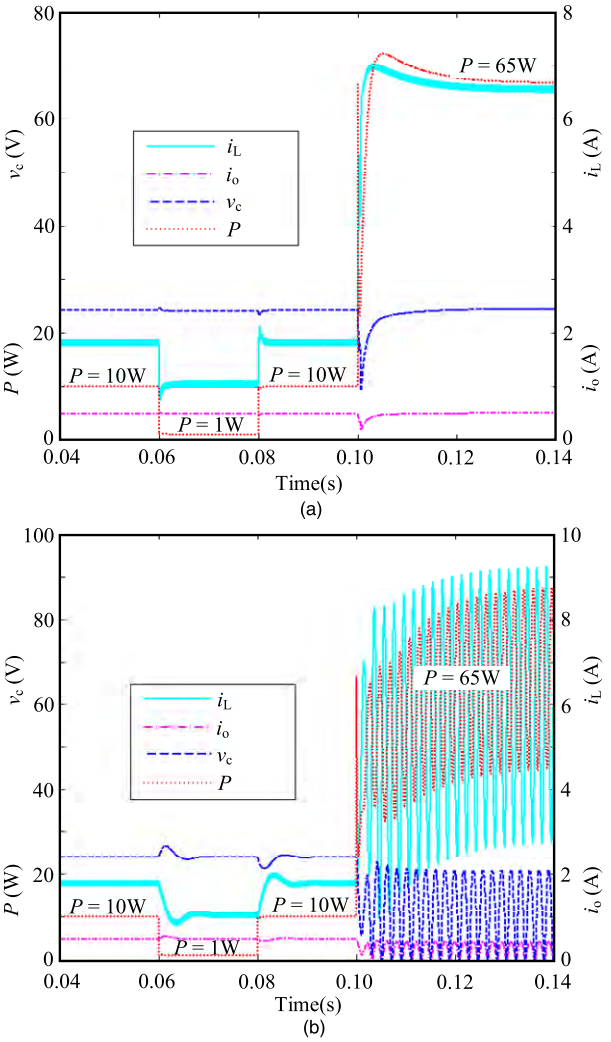

FIGURE 4. System dynamic response waveforms when CPL change. (a) Adaptive back-stepping sliding mode control. (b) Conventional double closed-loop PI control.

It can be seen that the capacitor voltage is stabilized at the set reference value of 24 V after two controllers are adjusted independently when P changes from 10 W to 1 W and 1 W to 10 W, thus maintaining the stability of the DC bus voltage, but the proposed control strategy has smaller overshoot and faster response speed compared with the conventional double closed-loop PI control method. The proposed control strategy still achieves the control objective and maintains system stability when P changes from 10 W to 65 W, whereas the conventional double closed-loop PI control method appears instability of DC bus voltage. Therefore, under large variation of a constant power, the proposed control strategy enables the system to have a better dynamic response speed and anti-interference ability.

Fig. 5 shows the dynamic response waveform of the system when V_{in} is hopped from 12 V to 22 V and 22 V to 15 V at 0.06 s and 0.08 s, respectively. It can be seen that at the moment of the input voltage jump, the DC bus voltage can be stabilized at the reference value of 24 V under two control

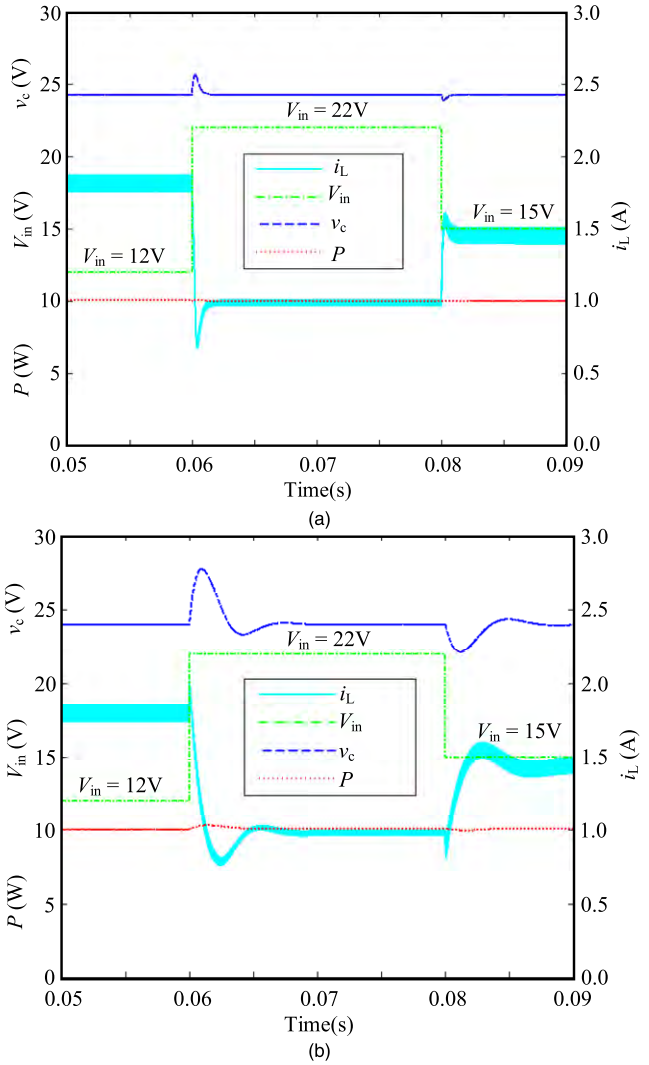

FIGURE 5. System dynamic response waveforms when input voltage change. (a) Adaptive back-stepping sliding mode control. (b) Conventional double closed-loop PI control.

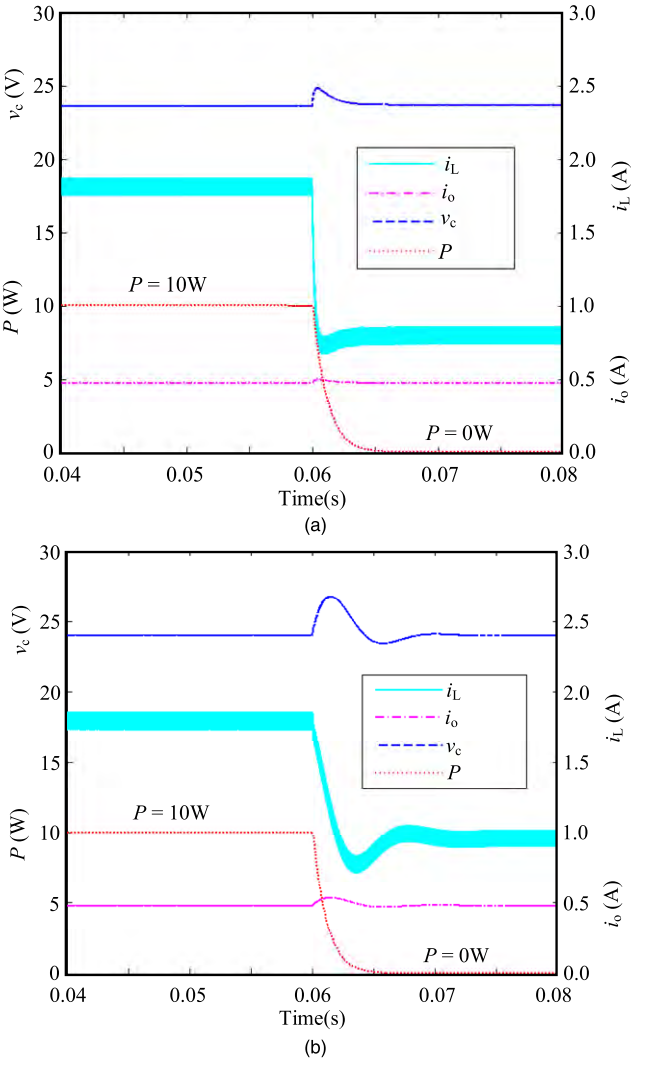

FIGURE 6. System dynamic response waveforms when CPL unload. (a) Adaptive back-stepping sliding mode control. (b) Conventional double closed-loop PI control.

strategies, providing a stable power of 10 W to the constant power load to ensure the stable operation of the system. However, it is not difficult to find by examining Fig. 5 that the proposed control strategy has no oscillation process and smaller overshoot compared with the conventional double closed-loop PI control method.

The robustness of the proposed control method and the conventional double closed-loop PI control method to uncertain factors is verified. Fig. 6 shows the dynamic response waveform of the system when CPL unload at 0.06 s. It can be seen that at the moment of the sudden unloading of the CPL, the CPL rapidly drops from 10 W to 0 W under two control strategies, and the capacitor voltage has a certain overshoot and then stabilizes at the reference value of 24 V to maintain the stability of the DC bus voltage. However, the proposed control strategy has better dynamic performance obviously compared with the conventional double closed-loop PI control method.

The worst-case scenario in which the system works, that is, only when the CPL is working, is considered. Fig. 7 shows the dynamic response waveform of the system when R unload and load at 0.07 s and 0.09s, respectively. As seen in Fig. 7, the DC bus voltage can be stabilized at the reference value of 24 V under two control strategies, the power of the CPL also has a certain fluctuation, but it can absorb a constant power of 10 W from the DC bus to maintain the stable operation of the CPL. However, the system has a faster response speed and a shorter adjustment time under the proposed control strategy. Therefore, the proposed control strategy can ensure that the system works more stable and has better anti-interference performance in the worst-case scenario compared with the conventional double closed-loop PI control method.

It is further verified that the adaptive mechanism effectively attenuates the effect of chatter on the system. Fig. 8 shows the system response waveform under pure

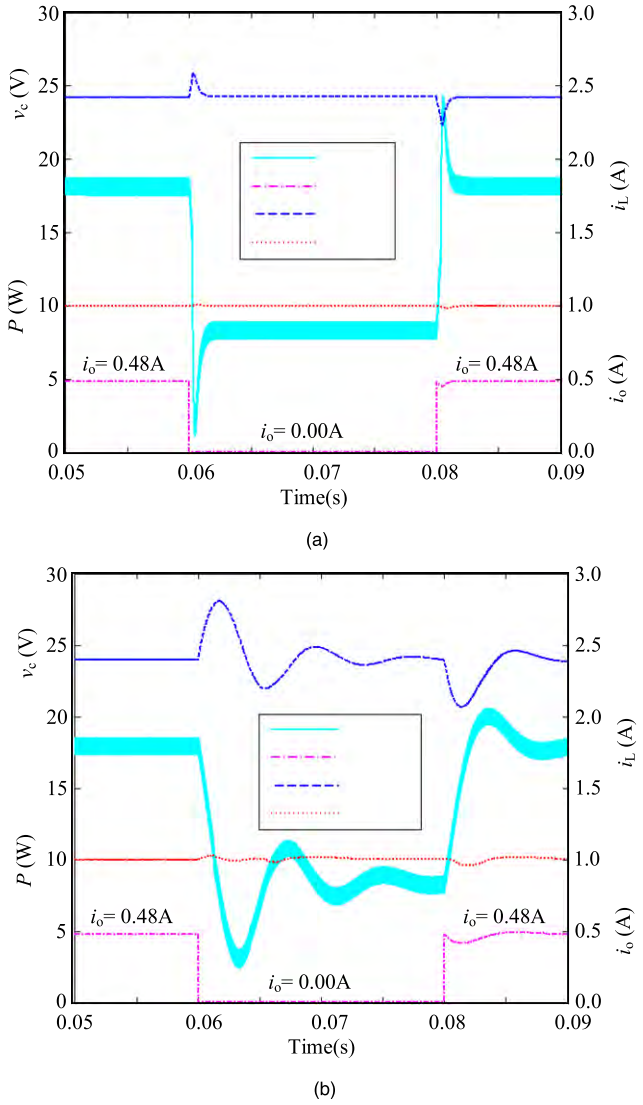

FIGURE 7. System dynamic response waveforms when resistive load unload and load. (a) Adaptive back-stepping sliding mode control. (b) Conventional double closed-loop PI control.

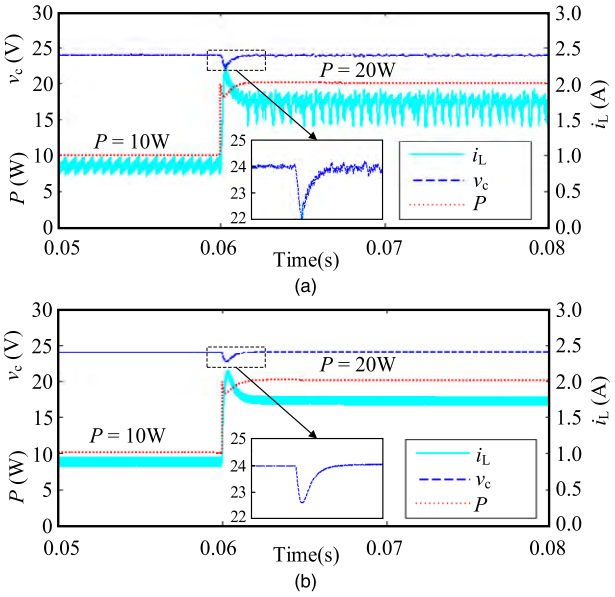

FIGURE 8. System response waveform when CPL changes. (a) $k_1 = 2000$. (b) Adaptive gain.

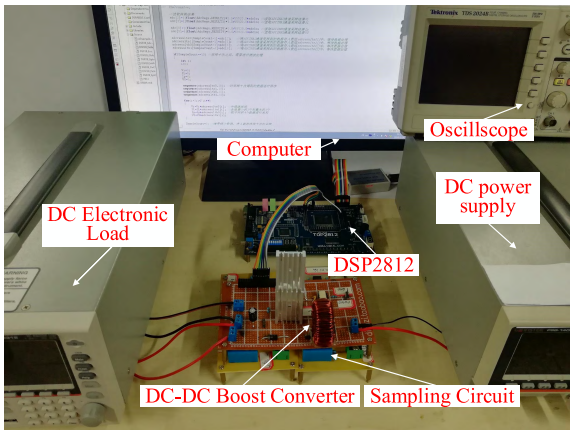

FIGURE 9. Experimental system setup.

CPL operation when $k_1 = 2000$, k_1 takes the adaptive gain shown in (31), and P jumps from 10 W to 20 W at 0.06 s. As seen in Fig. 8, the system can provide the required power for the CPL, and the capacitor voltage can be stabilized at the reference value of 24 V to maintain the stability of the DC bus voltage. However, it is not difficult to find by examining Fig. 8 that, under the adaptive parameters, both the bus voltage and the inductor current have smaller overshoots. For example, when P jumps, under the condition of $k_1 = 2000$, large oscillation occurs at the inductor current, the bus voltage has an overshoot of approximately 2 V. In comparison, under an adaptive gain, the inductor current has no obvious oscillation, and the bus voltage has an overshoot of just over 1 V. The chatter phenomenon of the system is thus greatly weakened, verifying the effectiveness of the introduced adaptive gain.

VI. EXPERIMENT

To further verify the correctness and effectiveness of the proposed nonlinear control strategy, a prototype machine as shown in Fig. 9 was built based on the control system shown in Fig. 3 for related experimental research, which consists of a GW Instek PSB-1400M mutil-range DC power supply, a GW Instek PEL-3031E programmable DC electronic load, DC/DC boost converter, a TMS320F2812 digital signal processor (DSP2812), sampling circuit and a Tektronix TDS 2024B four channel digital storage oscilloscope. IRF840 and TLP250 are used as switching device and gate drive circuit, respectively. CHB-25NP hall current sensor and CHV-25P hall voltage sensor are used for sampling current and voltage in the system, respectively. The control algorithm shown in Fig. 3 is implemented in DSP2812 to generate PWM signals for DC/DC boost converter. Parameters are the same as that listed in the simulation verification cases.

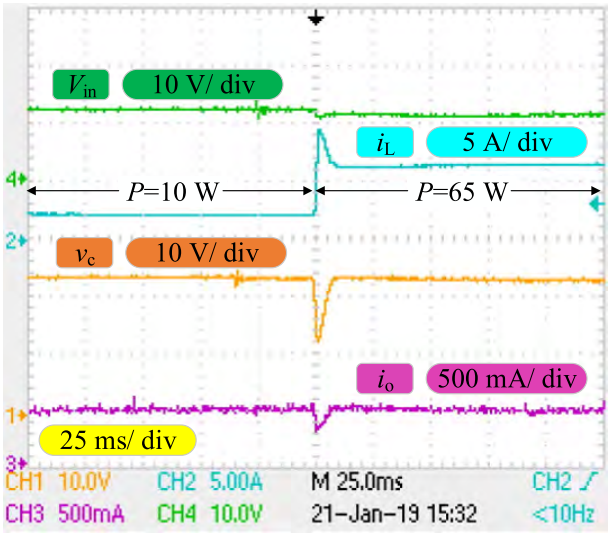

FIGURE 10. Experimental waveforms when CPL change.

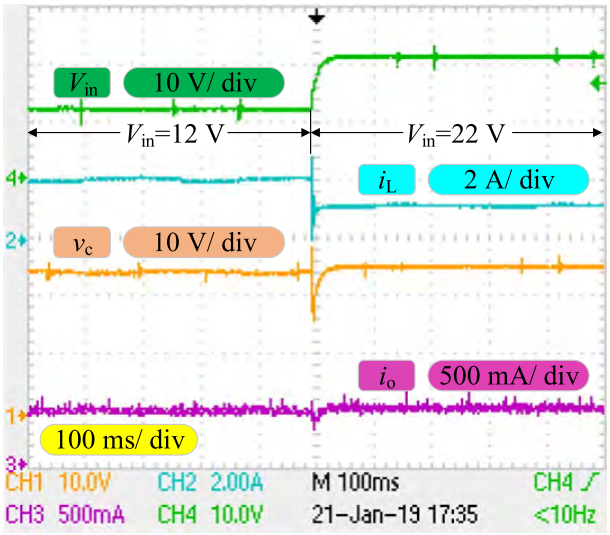

FIGURE 11. Experimental waveforms when input voltage change.

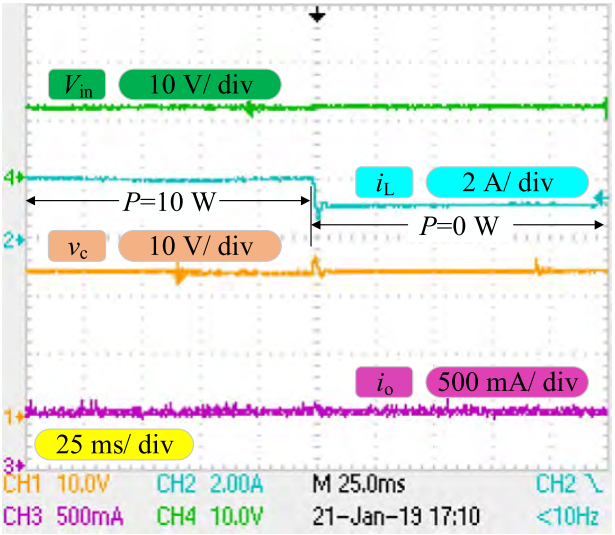

FIGURE 12. Experimental waveforms when CPL unload.

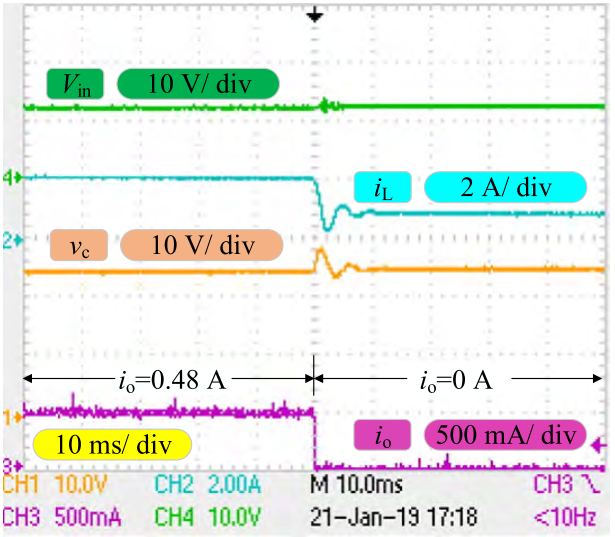

FIGURE 13. Experimental waveforms when resistive load unload.

To implement the proposed control algorithm in DSP2812, the algorithm (33) needs to be discretized in the program. As a very high sampling frequency would pose a heavy burden to the processor, the sampling is synchronized with the switching of the converter [37], thus the sampling period of the control system is 20 μs. The current and voltage are measured by the corresponding sensors and are converted through 12-bit analog-to-digital converters of the DSP2812. In order to improve the sampling accuracy, the current and the voltage are sorted, filtered and averaged in the program, respectively, and then the average values are taken as input value of the control algorithm.

Fig. 10 shows the experimental waveform of the system when P is hopped from 10 W to 65 W. It can be seen that at the moment of the CPL jump, the capacitor voltage has a certain overshoot but no oscillation, and it can stabilize at the reference value of 24 V after a regulation time of 10 ms, demonstrating a fast response speed. The proposed strategy achieves the control objective and maintains system stability under large variation of the constant power load.

Fig. 11 shows the experimental waveform of the system when input voltage is hopped from 12 V to 22 V. It can be seen that at the moment of the input voltage jump, the capacitor voltage has a certain overshoot, but it is stabilized at the set reference value of 24 V after a regulation time of 20 ms. The proposed strategy possesses a good robustness against power supply voltage variation.

Fig. 12 shows the experimental waveform of the system when CPL unload. It can be seen that the capacitor voltage has an overshoot of approximately 2 V, but it can stabilize at the reference value of 24 V after a regulation time of 5 ms, demonstrating a fast response speed.

Fig. 13 shows the experimental waveform of the system when R unload. It can be seen that at the moment of unloading the resistive load, the output current $i_o$is reduced from 0.48 A to 0 A. The capacitor voltage has a fluctuation, but it can be stabilized at the set value of 24 V to maintain the bus voltage.

However, the inductor current has a certain error between the experimental results and the simulation results. Further analysis indicates that during the simulation process, the switching device and the diodes are ideal, and the power consumption of the system by the voltage drop is not taken into account. However, in the actual circuit, the voltage drop and the loss of the sampling circuit are unavoidable, resulting in a small difference between the experimental waveform and the simulated waveform. Therefore, the experimental results are basically consistent with the simulation results, which verifies the correctness and effectiveness of the proposed control strategy.

VII. CONCLUSION

In this paper, a nonlinear control method combining the exact feedback linearization technique and the adaptive backstepping sliding mode control is proposed for boost converter with constant power load in DC microgrid. The proposed method has the following features:

1) The partial linearization of the nonlinear system is achieved by using the input-output exact feedback linearization technique. By studying the zero-dynamic stability of the system, it can be found that when the direct capacitor voltage is controlled, its zero dynamics are unstable, and the system is a non-minimum phase system. When the indirect inductor current is controlled, its zero dynamics are asymptotically stable, and the system is a minimum phase system.
2) On the basis of realizing the exact linearization of the system, an adaptive mechanism is introduced into the design of the backstepping sliding mode control algorithm, which solves the problem of a priori estimation of the upper-bound information of the disturbance and system parameter uncertainty and reduces the impact of chatter on the system.
3) The nonlinear control strategy proposed in this paper can be extended to other DC-DC converters with constant power loads such as buck and buck-boost converters. The controller is simple in design, easy to implement, and fully adaptive to changes in the circuit parameters.

Therefore, the proposed control method overcomes the shortcomings of the exact feedback linearization technique, including the dependency on accurate mathematical models and inapplicability to unstable zero dynamic systems, solves the instability problem caused by constant power loads, reduces the influence of sliding mode chatter on the system, and ensures the stability of the DC bus voltage.

REFERENCES

[1] A. P. N. Tahim, D. J. Pagano, E. Lenz, and V. Stramosk, "Modeling and stability analysis of islanded DC microgrids under droop control," *IEEE Trans. Power Electron.*, vol. 30, no. 8, pp. 4597–4607, Aug. 2015.
[2] G. Sulligoi, D. Bosich, G. Giadrossi, L. Zhu, M. Cupelli, and A. Monti, "Multiconverter medium voltage DC power systems on ships: Constant-power loads instability solution using linearization via state feedback control," *IEEE Trans. Smart Grid*, vol. 5, no. 5, pp. 2543–2552, Sep. 2014.
[3] A. M. Rahimi, G. A. Williamson, and A. Emadi, "Loop-cancellation technique: A novel nonlinear feedback to overcome the destabilizing effect of constant-power loads," *IEEE Trans. Veh. Technol.*, vol. 59, no. 2, pp. 650–661, Feb. 2010.
[4] L. Herrera, W. Zhang, and J. Wang, "Stability analysis and controller design of DC microgrids with constant power loads," *IEEE Trans. Smart Grid*, vol. 8, no. 2, pp. 881–888, Mar. 2017.
[5] S. Liu, P. Su, and L. Zhang, "A virtual negative inductor stabilizing strategy for DC microgrid with constant power loads," *IEEE Access*, vol. 6, pp. 59728–59741, 2018.
[6] M. N. Hussain, R. Mishra, and V. Agarwal, "A frequency-dependent virtual impedance for voltage-regulating converters feeding constant power loads in a DC microgrid," *IEEE Trans. Ind. Appl.*, vol. 54, no. 6, pp. 5630–5639, Nov./Dec. 2018.
[7] E. Hossain, R. Perez, A. Nasiri, and S. Padmanaban, "A comprehensive review on constant power loads compensation techniques," *IEEE Access*, vol. 6, pp. 33285–33305, 2018.
[8] A. Isidori, A. J. Krener, C. Gori-Giorgi, and S. Monaco, "Nonlinear decoupling via feedback: A differential geometric approach," *IEEE Trans. Autom. Control*, vol. AC-26, no. 2, pp. 331–345, Apr. 1981.
[9] P. Liutanakul, S. Pierfederici, and F. Meibody-Tabar, "Application of SMC with I/O feedback linearization to the control of the cascade controlled-rectifier/inverter-motor drive system with small DC-link capacitor," *IEEE Trans. Power Electron.*, vol. 23, no. 5, pp. 2489–2499, Sep. 2008.
[10] T.-S. Lee, "Input-output linearization and zero-dynamics control of three-phase AC/DC voltage-source converters," *IEEE Trans. Power Electron.*, vol. 18, no. 1, pp. 11–22, Jan. 2003.
[11] S. Arora, T. P. Balsara, and K. D. Bhatia, "Input–output linearization of a boost converter with mixed load (constant voltage load and constant power load)," *IEEE Trans. Power Electron.*, vol. 34, no. 1, pp. 815–825, Jan. 2019.
[12] A. M. Boker and H. K. Khalil, "Semi-global output feedback stabilization of non-minimum phase nonlinear systems," *IEEE Trans. Autom. Control*, vol. 62, no. 8, pp. 4005–4010, Aug. 2016.
[13] Y. Li, K. R. Vannorsdel, A. J. Zirger, M. Norris, and D. Maksimovic, "Current mode control for boost converters with constant power loads," *IEEE Trans. Circuits Syst. I, Reg. Papers*, vol. 59, no. 1, pp. 198–206, Jan. 2012.
[14] T. Dragičević, "Dynamic stabilization of DC microgrids with predictive control of point-of-load converters," *IEEE Trans. Power Electron.*, vol. 33, no. 12, pp. 10872–10884, Dec. 2018.
[15] J. Zeng, Z. Zhang, and W. Qiao, "An interconnection and damping assignment passivity-based controller for a DC–DC boost converter with a constant power load," *IEEE Trans. Ind. Appl.*, vol. 50, no. 4, pp. 2314–2322, Jul./Aug. 2014.
[16] J. A. Solsona, S. G. Jorge, and C. A. Busada, "Nonlinear control of a buck converter which feeds a constant power load," *IEEE Trans. Power Electron.*, vol. 30, no. 12, pp. 7193–7201, Dec. 2015.
[17] M. Cespedes, L. Xing, and J. Sun, "Constant-power load system stabilization by passive damping," *IEEE Trans. Power Electron.*, vol. 26, no. 7, pp. 1832–1836, Jul. 2011.
[18] P. Magne, B. Nahid-Mobarakeh, and S. Pierfederici, "Active stabilization of DC microgrids without remote sensors for more electric aircraft," *IEEE Trans. Ind. Appl.*, vol. 49, no. 5, pp. 2352–2360, Sep. 2013.
[19] P. Magne, D. Marx, B. Nahid-Mobarakeh, and S. Pierfederici, "Large-signal stabilization of a DC-link supplying a constant power load using a virtual capacitor: Impact on the domain of attraction," *IEEE Trans. Ind. Appl.*, vol. 48, no. 3, pp. 878–887, May/Jun. 2012.
[20] M. A. Kardan *et al.*, "Improved stabilization of nonlinear DC microgrids: Cubature Kalman filter approach," *IEEE Trans. Ind. Appl.*, vol. 54, no. 5, pp. 5104–5112, Sep. 2018.
[21] Q. Xu, C. Zhang, C. Wen, and P. Wang, "A novel composite nonlinear controller for stabilization of constant power load in DC microgrid," *IEEE Trans. Smart Grid*, vol. 10, no. 1, pp. 752–761, Jan. 2019. doi: 10.1109/TSG.2017.2751755.

[22] Y. Zhao, W. Qiao, and D. Ha, "A sliding-mode duty-ratio controller for DC/DC buck converters with constant power loads," *IEEE Trans. Ind. Appl.*, vol. 50, no. 2, pp. 1448–1458, Mar. 2014.
[23] S. Singh, D. Fulwani, and V. Kumar, "Robust sliding-mode control of DC/DC boost converter feeding a constant power load," *IET Power Electron.*, vol. 8, no. 7, pp. 1230–1237, Jul. 2015.
[24] M. Zhang, Y. Li, F. Liu, L. Luo, Y. Cao, and M. Shahidehpour, "Voltage stability analysis and sliding-mode control method for rectifier in DC systems with constant power loads," *IEEE Trans. Emerg. Sel. Topics Power Electron.*, vol. 5, no. 4, pp. 1621–1630, Dec. 2017.
[25] S. H. Chincholkar, W. Jiang, and C.-Y. Chan, "A modified hysteresis-modulation-based sliding mode control for improved performance in hybrid DC–DC boost converter," *IEEE Trans. Circuits Syst. II, Exp. Briefs*, vol. 65, no. 11, pp. 1683–1687, Nov. 2018.
[26] A. Emadi, A. Khaligh, C. H. Rivetta, and G. A. Williamson, "Constant power loads and negative impedance instability in automotive systems: Definition, modeling, stability, and control of power electronic converters and motor drives," *IEEE Trans. Veh. Technol.*, vol. 55, no. 4, pp. 1112–1125, Jul. 2006.
[27] L. Benadero, R. Cristiano, D. J. Pagano, and E. Ponce, "Nonlinear analysis of interconnected power converters: A case study," *IEEE J. Emerg. Sel. Topics Circuits Syst.*, vol. 5, no. 3, pp. 326–335, Sep. 2015.
[28] H. N. Jazi, A. Goudarzian, R. Pourbagher, and S. Y. Derakhshandeh, "PI and PWM sliding mode control of POESLL converter," *IEEE Trans. Aerosp. Electron. Syst.*, vol. 53, no. 5, pp. 2167–2177, Oct. 2017.
[29] Q. Su, W. Quan, G. Cai, and J. Li, "Improved adaptive backstepping sliding mode control for generator steam valves of non-linear power systems," *IET Control Theory Appl.*, vol. 11, no. 9, pp. 1414–1419, Jun. 2017.
[30] F. Chen, R. Jiang, K. Zhang, B. Jiang, and G. Tao, "Robust backstepping sliding-mode control and observer-based fault estimation for a quadrotor UAV," *IEEE Trans. Ind. Electron.*, vol. 63, no. 8, pp. 5044–5056, Aug. 2016.
[31] M. Wu and D. D.-C. Lu, "A novel stabilization method of LC input filter with constant power loads without load performance compromise in DC microgrids," *IEEE Trans. Ind. Electron.*, vol. 62, no. 7, pp. 4552–4562, Jul. 2015.
[32] F. Dong, X. Lei, and W. Chou, "A dynamic model and control method for a two-axis inertially stabilized platform," *IEEE Trans. Ind. Electron.*, vol. 64, no. 1, pp. 432–439, Jan. 2017.
[33] S. Singh, V. Kumar, and D. Fulwani, "Mitigation of destabilising effect of CPLs in island DC micro-grid using non-linear control," *IET Power Electron.*, vol. 10, no. 3, pp. 387–397, Oct. 2017.
[34] O. Barambones, P. Alkorta, A. J. Garrido, I. Garrido, and F. J. Maseda, "An adaptive sliding mode control scheme for induction motor drives," *Int. J. Circuits, Syst. Signal Process.*, vol. 1, no. 1, pp. 73–78, 2007.
[35] J. Y. Hung, W. Gao, and J. C. Hung, "Variable structure control: A survey," *IEEE Trans. Ind. Electron.*, vol. 40, no. 1, pp. 2–22, Feb. 1993.
[36] S. Bacha, L. Munteanu, and A. L. Bratcu, "Power electronic converters modeling and control," in *Advanced Textbooks in Control and Signal Processing*, vol. 454. London, U.K.: Springer, 2014.
[37] D. M. V. D. Sype, K. D. Gusseme, A. P. V. D. Bossche, and J. A. A. Melkebeek, "A sampling algorithm for digitally controlled boost PFC converters," *IEEE Trans. Power Electron.*, vol. 19, no. 3, pp. 649–657, May 2004.

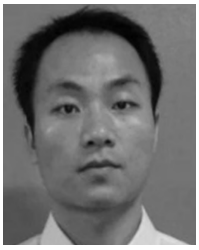

JIARONG WU was born in Nanning, China, in 1988. He received the B.S. degree in electrical and information engineering from Wuzhou University, Wuzhou, in 2013, and the M.S. degree from Guangxi University, Nanning, in 2016, where he is currently pursuing the Ph.D. degree. His research interests include nonlinear control and applications in power electronics.

YIMIN LU (M'16) received the B.S. degree in measurement technology and instrumentation from Southeast University, Nanjing, in 1992, the M.S. degree from Guangxi University, Nanning, in 2000, and the Ph.D. degree in control theory and control engineering from the South China University of Technology, Guangzhou, in 2004. She joined the School of Electrical Engineering, Guangxi University, as a Teaching Assistant, in 1992, where she is currently a Professor. From 2007 to 2008, she was a Postdoctoral Researcher with the Department of Electronic and Electrical Engineering, University of Sheffield, U.K. From 2014 to 2015, she was a Visiting Research Scholar with the Department of Mechanical Engineering and WEMPEC, University of Wisconsin–Madison, USA. Her research interest includes control theory and applications in power electronics.